ELSEVIER

Journal of Nuclear Materials 307–311 (2002) 610–614

journal of nuclear materials

www.elsevier.com/locate/jnucmat

High temperature performance of highly purified V–4Cr–4Ti alloy, NIFS-Heat1

K. Fukumoto *, T. Yamamoto, N. Nakao, S. Takahashi, H. Matsui

Institute for Materials Research, Tohoku University, Katahira 2-1-1, Aoba-ku, Sendai 980-8577, Japan

Abstract

High temperature performance tests including tensile, creep and creep-fatigue tests were conducted using specimens from a large ingot of highly purified V–4Cr–4Ti alloys, NIFS-Heat1. The obtained tensile data of NIFS-Heat1 alloys agree well with previous V–4Cr–4Ti alloys data. The most significant effect for the impurity reduction in NIFS-Heat1 alloys was the higher temperature for the appearance of the dynamic strain hardening compared to previous heats of V–4Cr–4Ti. From uniaxial creep tests, a creep-stress exponent of the NIFS-Heat1 alloy is about 5–8 and the characteristic of creep mechanism is the dislocation creep in pure metals. The apparent activation energies of creep deformation ranged from 180 to 210 kJ/mol at a temperature regime from 750 to 800 °C. No significant degradation due to fatigue behavior was observed during creep-fatigue tests. The creep-fatigue behavior was superior to the load-constant creep behavior in the same stress and temperature conditions at a lower stress condition.

1. Introduction

Vanadium-base alloys are promising candidates for fusion reactor applications because of their low-activation and good thermal mechanical properties and radiation resistance at high temperature. But susceptibility of vanadium base alloys to low temperature embrittlement during neutron irradiation may limit the application of these alloys in low temperature (<400 °C) regimes. The radiation-induced loss of ductility at <400 °C may be attributed to fine precipitates containing C, O and N [1–3]. The reduction of these elements is expected to improve the radiation resistance of the alloys at low temperature.

The National Institute for Fusion Science (NIFS), in collaboration with Japanese industry has initiated a program to fabricate a large ingot of highly purified V–4Cr–4Ti alloys. A medium size (≃30 kg) ingot of V–4Cr–4Ti was fabricated by EB and VAR methods, which was designated as NIFS-Heat1. The impurity level for fabricating large V–Cr–Ti ingots was achieved as ≃60 wppm C, ≃180 ppm O, ≃100 wppm N and 1 wppm or less of metallic elements.

The objective of this study is to determine the baseline tensile, creep and creep-fatigue properties of NIFS-Heat1 of highly purified V–4Cr–4Ti alloys and make clear how much impurity levels affect the mechanical properties especially at high temperature.

2. Experimental procedure

The chemistry of a NIFS-Heat1 of V–4Cr–4Ti alloy has been previously reported [4]. SSJ specimens ($16 \times 4 \times 0.25$ mm^3 with a 1.2 mm × 5 mm gauge section) were punched out from the sheets and annealed at 950 or 1000 °C for 2 h after degassing treatment at 600 °C for 0.5 h in a vacuum $< 1 \times 10^{-4}$ Pa. Tensile tests were carried out at a strain rate of 6.67×10^{-4}/s at temperatures ranging from room temperature to 800 °C in a vacuum $< 1 \times 10^{-4}$ Pa. In order to get information of the strain rate sensitivity (SRS) [5], tensile tests were done at room temperature for strain rates in the range

* Corresponding author. Tel.: +81-22 215 2067; fax: +81-22 215 2066.

E-mail address: fukumoto@imr.tohoku.ac.jp (K. Fukumoto).

0022-3115/02/$ - see front matter
PII: S0022-3115(02)01216-3

6.67×10^{-4} to 6.67×10^{-2}/s. Creep and creep-fatigue tests were carried out on the same machine as the tensile tests, which was converted into a load-controlled configuration. The specimen shape was the SSJ type. The temperatures of the creep tests were 700, 750 and 800 °C with applied stress levels of 150 and 200 MPa. The fluctuation of the applied stress was within 3 MPa for each test. The temperature of creep-fatigue tests was 800 °C with applied stress levels of 150 and 200 MPa. The cyclic mode of the creep-fatigue tests was adopted as a rectangular pulse with a period of 2 h. The initial degree of vacuum was about 2×10^{-4} Pa at 800 °C and the final ultimate one was about 1×10^{-6} Pa after a 100 h creep test. No pick-up of gas impurity during creep and creep-fatigue tests could be detected from chemical analysis before and after tests.

3. Results and discussion

3.1. Tensile tests

The results of tensile tests are shown in Fig. 1. The data from this study are compared to previous data [5–15] for trending purpose. The difference of annealing temperature of both 950 and 1000 °C for NIFS-Heat1 cannot be seen clearly. The obtained data compare and agree well with previous reported data. Yield strength and ultimate tensile strength of the NIFS-Heat1 are slightly lower and the uniform elongation is slightly greater than the group average. The deviations from group average may be caused by the reduction of interstitial impurity level mainly.

Data of the SRS were also determined at room temperature and the lower yield stress exhibits a positive SRS, for strain rates in the range 10^{-4} to 10^{-2}/s. The hardening strain rate sensitivity, m, were 0.040 and 0.016 for a 950 °C annealed and a 1000 °C annealed one, respectively. The m value of US heat, #832665 annealed at 1000 °C for 2 h was 0.019 [15] and it was in good agreement with our work. The difference in m value between the 950 °C annealed one and the 1000 °C annealed one is still unclear. The distribution of precipitates and the levels of interstitial impurities in solute may affect the behavior of dislocation motion during the Luders extension in tensile tests and contribute to the difference in SRS behavior between different heat treatments.

Fig. 2 shows the variation of serration magnitude with test temperatures for 950 °C annealed and 1000 °C annealed NIFS-Heat1 alloys and a #832665 V–4Cr–4Ti alloy in the previous work. The serrations of USA heat start appearing with increase in temperature above 400 °C [12,15], however those of NIFS-Heat1 start appearing at 500 °C. Dynamic strain aging due to solute atoms and interstitial impurities has been identified as the probable cause for the appearance of serrations in the stress strain curves of many alloys [16–18]. A relationship between strain rate ε and diffusivity of interstitial atoms D is described as $\varepsilon = 10^9 D$ for calculating the minimum temperature for serrated yielding [16]. D is given by $D = D_0 \exp(-Q/RT)$, where D_0 is the diffusion coefficient, Q is the activation energy. This equation can be used to estimate the minimum temperatures for serrated yielding for the impurity interstitials, oxygen, carbon and nitrogen [12,15,17]. By using the value of diffusion coefficient and activation energy of impurity interstitial atoms, the onset of serration temperature for each interstitial element can be obtained. By using the strain rate value of 6.67×10^{-4}/s in this study, the onset

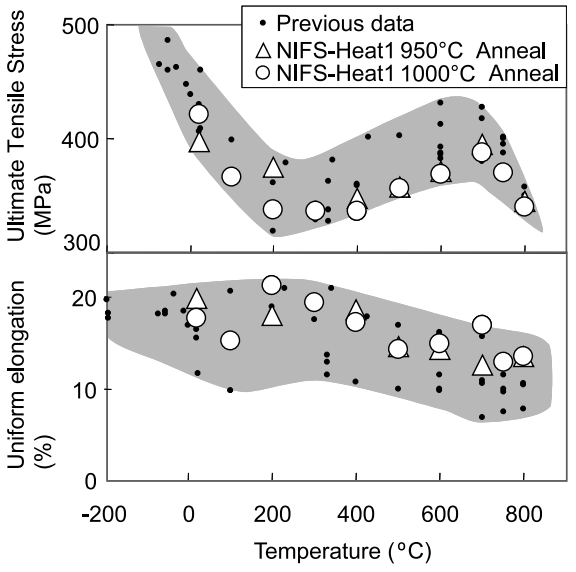

Fig. 1. Test temperature dependence of ultimate tensile strength and uniform elongation data for the NIFS-Heat1 alloys annealed at 950 and 1000 °C in comparison with the previous data.

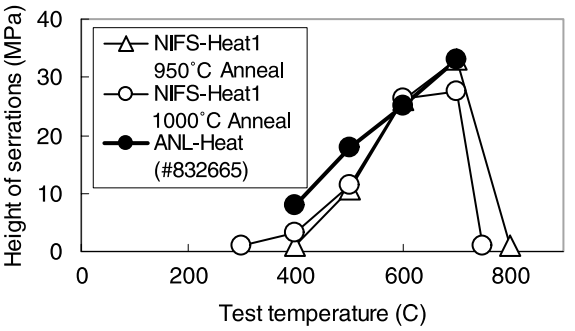

Fig. 2. The variation in height of serrations with test temperature for the NIFS-Heat1 alloys annealed at 950 and 1000 °C, and the ANL-Heat (#832665).

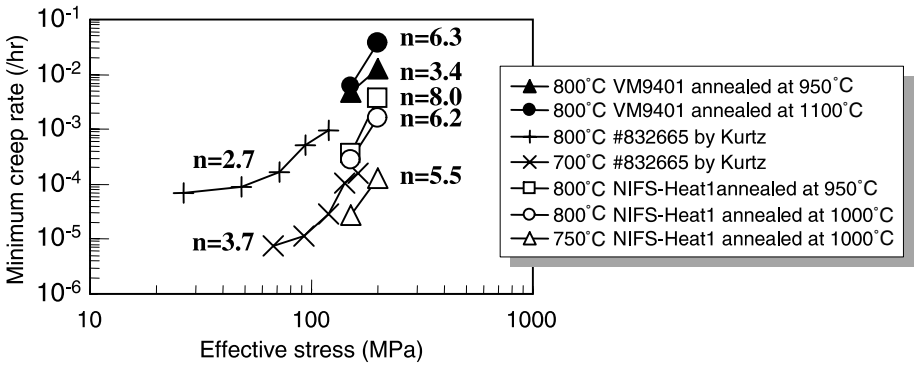

Fig. 3. Stress dependence of the minimum creep rate of NIFS-Heat1 alloys and previous works.

temperatures determined for oxygen, carbon, and nitrogen are 355, 336 and 463 °C, respectively. It is suggested that the serrations in the stress–strain curves of the #832665 heat is related to mobility of oxygen. On the other hand, the serrations of NIFS-Heat1 cannot be seen at 400 °C so that there is no oxygen migration for dynamic strain aging in NIFS-Heat1. This is caused by the reduction of oxygen contents in matrix. The serrations of NIFS-Heat1 are related to mobility of nitrogen above 500 °C. This is a significant effect of impurity reduction in NIFS-Heat1 apparently.

3.2. Creep tests

The strain–time curves for creep tests of NIFS-Heat1 alloys were obviously divided into three regimes: a primary creep regime (transient creep), a secondary creep regime (steady state creep) and a tertiary creep regime (acceleration creep). Secondary creep rates were determined by fitting a straight regime on the secondary creep regime containing the minimum rate with the method of least squares. The shape of creep curve is one of the familiar characteristics of uniaxial creep tests [19], while biaxial creep tests in the previous works using pressurized tubes did not show evidence of primary and secondary creep [20].

Fig. 3 shows a comparison of steady state creep rate for NIFS-Heat1 annealed at 1000 °C as a function of stress. All of the data in Fig. 3 were fitted to a equation $d\varepsilon/dt = A\sigma^n$, where A is a constant and n is the stress exponent. The stress exponent is ranged from 5 to 9 for 700, 750 and 800 °C creep data. There have been reported that the strain exponents, n for pure V and V–Ti alloys [21–23] are beyond five on the similar creep test conditions in this work. On the other hand, Kurtz has reported [20] that n in biaxial creep tests for ANL-heat; #832665 is between 2.7 and 3.7 in the same range of stress as this work. As a pre-creep test for NIFS-Heat1 alloy in this work, creep tests for a VM9401 heat of V-alloy [7] have been done and the strain exponent, n was 3.4 and 6.8 for VM9401 annealed at 950 and 1100 °C, respectively. The tensile behavior and chemical composition between VM9401 and #832665 heat are so similar that the difference in stress exponent is not due to geometry of specimens, but is characteristic of creep in vanadium alloys. For experimentally observed stress dependence of creep rate of pure metals when the creep is controlled by lattice diffusion, the stress exponent $n \approx 5$ is typical [24]. Therefore, the characteristic of creep behavior in the NIFS-Heat1 alloy should be the dislocation creep in pure metals even though V–Cr–Ti alloys are solid solution alloys. Fig. 4 is plotted as log strain rate vs. reciprocal temperature for NIFS-Heat1. The apparent activation energies determined from the slop in this plot and 211 and 185 kJ/mol was obtained for the stressed one at 200 MPa and at 150 MPa, respectively. These values are lower than the activation energy of ANL-Heat #832665, 299 kJ/mol [20], and higher than that of V–2.8Ti, 125 kJ/mol [22,25]. According to previous works, the strong scavenging effect of titanium and low oxygen solubility in V–Ti correspond to the lowest activation energy of creep rate in V–Ti system alloys. It means the oxygen contents may be quite lower in V–3Ti than any other V–Ti system alloys

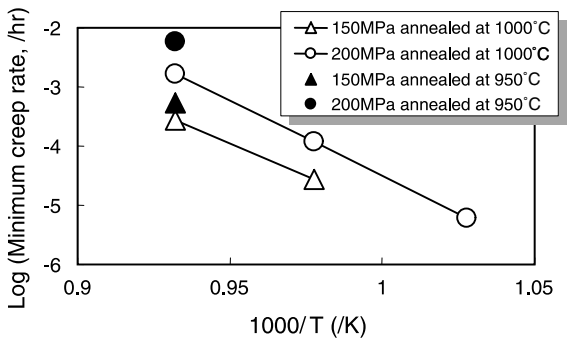

Fig. 4. Arrehnius plot of minimum creep rates for NIFS-Heat1 alloys.

and the reduction of matrix impurity may lead to a lower activation energy. The activation energies for NIFS-Heat1 also should be lower than ones of the previous V–4Cr–4Ti alloys because of the reduction in oxygen and interstitial impurities. The relations between creep stress and Larson-Miller parameter in comparison with the previous data [19,22,25–29] are plotted as Fig. 5. The Larson–Miller parameter was estimated using following equation; $P = T(C + \log t_b)$, where T is the temperature (K), t_b is rupture time (h) and C is a constant characteristic of the alloy which usually has a value of 20. The data of this work are in close agreement with the previous data of other V–4Cr–4Ti alloys. The creep strength of a V–(3–5)wt%Ti alloy with the lowest activation energy must be stronger than any other V–Ti binary alloys, according to the previous works [22]. The difference between V–3Ti alloys and NIFS-Heat1 maybe caused by the distribution of Ti-precipitates, because the density and the size of Ti-precipitates are large around V–3Ti alloys as a function of Ti element in V–Ti system, therefore the levels of interstitial impurities are quite low in V–3Ti alloys [27]. However though the large creep strength of V–3Ti may be due to precipitate dispersion strengthening [22,25,29], it is not reflected in the case of NIFS-Heat1 due to lack of the precipitates. Hence, The impurity level of NIFS-Heat1, 150–300 wppm of interstitial impurity is not low enough to reduce the thermal creep property since interstitial impurities in solute in NIFS-Heat1 still preserve the pinning effect for the dislocation motion or retard the vacancy diffusion during creep test at 800 °C as trapping sites. Consequently, the thermal creep property of NIFS-Heat1 alloys is comparable to other V–4Cr–4Ti alloys and the impurity level (150–300 wppm) does not affect the thermal creep property in the V–4Cr–4Ti systems so much, at least for short-term (~100 h) medium-high stress tests.

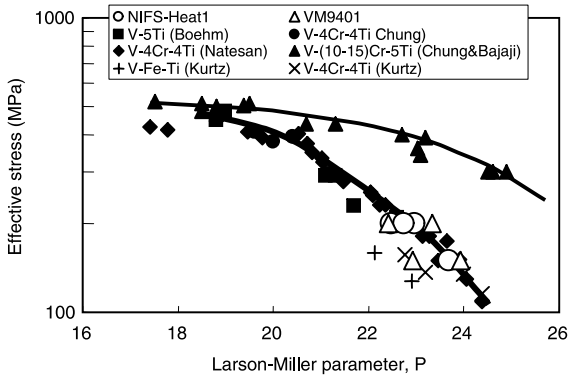

Fig. 5. Larson–Miller parameter correlation for creep-rupture of NIFS-Heat1 in comparison with the previous works of V–4Cr–4Ti and V–(10–15)Cr–5Ti.

3.3. Creep-fatigue tests

Fig. 6 shows the creep-strain curves in the constant creep test and the creep-fatigue test at 800 °C with stress levels of 150 and 200 MPa. The curves of unloading part were excluded from the curves in the creep-fatigue strain curves. The rupture time of both the creep and the creep-fatigue test at a stress level of 200 MPa were almost same and those strain curves were divided into three stages. Minimum creep rate of creep test and creep-fatigue test was 0.16%/h and 0.3%/h, respectively. From the viewpoint of creep rate, the creep-fatigue behavior seems to accelerate the deformation process compared to constant-load test. On the other hand, the strain curve in the creep-fatigue test at a stress level of 150 MPa was different from the creep tests. The rupture time of the creep-fatigue test was larger than creep test, and the minimum creep rate of creep fatigue-test and creep test was 0.015%/h and 0.028%/h, respectively. It is indicated that the creep-fatigue behavior is superior to constant-load creep behavior at lower stress level. The main reason why the difference of the creep-fatigues behavior between at 150 and 200 MPa can be explained by the strain behavior per

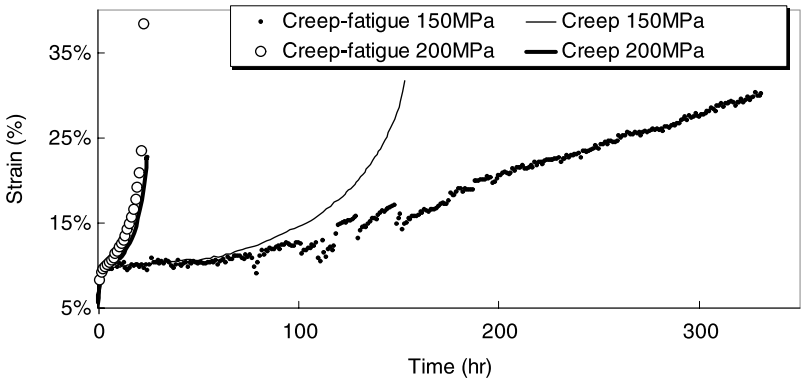

Fig. 6. Creep-strain curve on both creep and creep-fatigue tests. The creep curves are drawn with lines and the creep-fatigue curves with small circles.

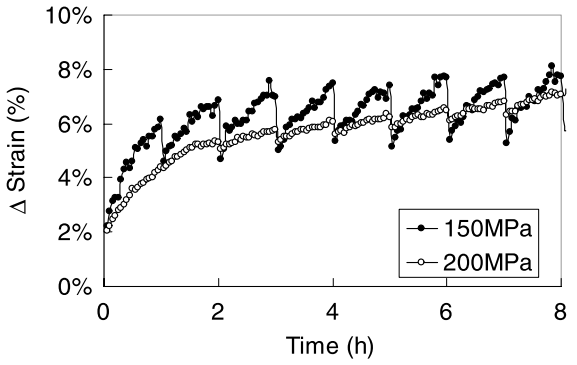

Fig. 7. The difference between creep-fatigue test at 150 and 200 MPa. The data are plotted with relative time as abscissa against relative amount of strain as ordinate. The data of 200 MPa were taken from the steady state regime after transient creep, for 3rd to 8th h, and the data of 150 MPa were taken from the steady state regime, for 10th to 15th h.

fatigue cycle. The essential difference between creep-fatigue test at 150 MPa and at 200 MPa is illustrated in Fig. 7. The strain curve at 150 MPa shows the rapid decreases of creep elongation after loading and significant increases of strain during loading compared with 200 MPa. The tendency can be seen in the stage I and stage II creep regime in creep-fatigue test at 150 MPa. The significant increases during loading is an indication that the transient creep strains appeared during loading and the microstructure did not developed into steady state creep microstructures such as dislocation cell structures. The small drop of elongation after unloading at 200 MPa shows the microstructural evolution in creep-fatigue test at 200 MPa is in the steady state creep stage, stage II. Hence the creep rate of creep-fatigue test at 150 MPa is smaller than that of constant-load creep test. From these tests and from creep-fatigue literature, the interval of creep-fatigue test on loading is an important parameter controlling the creep-fatigue lifetime. More research work on creep-fatigue tests is required in order to make clear what factor is important in controlling the creep-fatigue behavior of vanadium alloys.

4. Conclusions

High temperature performance tests were conducted using specimens from a large ingot of highly purified V–4Cr–4Ti alloys, NIFS-Heat1. The obtained tensile data agree well with previous reported data. Yield strength and ultimate tensile strength of the NIFS-Heat1 are slightly lower and the uniform elongation is slightly greater than the V–4Cr–4Ti group average. The most significant effect for impurity reduction appeared in the serration behavior on stress strain curve already known as the effect of dynamic strain aging hardening. The onset temperature of serration was increased (vs. ~300 °C in US heat) to 500 °C due to the reduction of oxygen concentration in the NIFS-Heat1 alloy.

The creep-stress exponent of NIFS-Heat1 alloys is about 5–8 and the characteristic of creep mechanism is the dislocation creep in pure metals. The apparent activation energies for creep deformation ranged from 180 to 210 kJ/mol at a stress level from 150 to 200 MPa in the temperature regime from 750 to 800 °C.

From the creep-fatigue test in place of thermal fatigue, significant degradation due to fatigue behavior was not observed. In the creep-fatigue test with lower stress, the creep-fatigue behavior was superior to constant-load creep behavior at the same stress and temperature conditions.

References

[1] M. Satou, T. Chuto, K. Abe, J. Nucl. Mater. 283–287 (2000) 367.
[2] K. Fukumoto, H. Matsui, et al., J. Nucl. Mater. 283–287 (2000) 535.
[3] P.M. Rice, S.J. Zinkle, J. Nucl. Mater. 258–263 (1998) 1414.
[4] T. Muroga, T. Nagasaka, et al., J. Nucl. Mater. 283–287 (2000) 711.
[5] A.F. Rowcliffe, S.J. Zinkle, D.T. Hoelzer, J. Nucl. Mater. 283–287 (2000) 508.
[6] T.S. Bray, H. Tsai, L.J. Nowicki, et al., J. Nucl. Mater. 283–287 (2000) 633.
[7] K. Fukumoto, T. Morimura, T. Tanaka, et al., J. Nucl. Mater. 239 (1996) 170.
[8] M.C. Billone, H.M. Chung, D.L. Smith, J. Nucl. Mater. 258–263 (1998) 1523.
[9] H. Tsai et al., DOE/ER-0313/25 (1998) 3.
[10] S.J. Zinkle et al., DOE/ER-0313/24 (1998) 11.
[11] H.M. Chung et al., DOE/ER-0313/19 (1995) 17.
[12] A.N. Gubbi et al., DOE/ER-0313/20 (1996) 38.
[13] S.J. Zinkle et al., DOE/ER-0313/23 (1997) 99.
[14] D.T. Hoelzer et al., J. Nucl. Mater. 283–287 (2000) 616.
[15] A.F. Rowcliffe et al., DOE/ER0313/26 (1999) 25.
[16] A.H. Cottrell, Philos. Mag. 44 (1953) 829.
[17] J.W. Edington, T.C. Lindley, R.E. Smallman, Acta Metall. 12 (1964) 1025.
[18] M.S. Wechsler, K.L. Murty, Metall. Trans. A. 20A (1989) 2637.
[19] K. Natesan et al., this Conference, ICFRM-10.
[20] R.J. Kurtz, M.L. Hamilton, J. Nucl. Mater. 283–287 (2000) 628.
[21] K.R. Wheeler et al., Acta Metall. 19 (1971) 21.
[22] H. Boehm et al., J. Less-Common Met. 12 (1967) 280.
[23] T. Kainuma et al., J. Less-Common Met. 86 (1982) 263.
[24] J. Cadek, in: Creep in metallic materials, Elsevier, Amsterdam, 1988, p. 115.
[25] H. Boehm et al., Z. Metallkde. 59 (1968) 715.
[26] H.M. Chung et al., J. Nucl. Mater. 212–215 (1994) 772.
[27] K.H. Kramer, J. Less-Common Met. 21 (1970) 365.
[28] R. Bajaji et al., DOE/ER0045/10 (1983) 74.
[29] D. Harrod, R.E. Gold, Int. Met. Rev. 25 (1980) 163.